

Strength and Fracture of Silicon Wafers Reactively Bonded by Al/Ni Rapid Heating

Sarankamol Athichaikhongphat,¹ Kana Maekawa,¹ Amit Banerjee,¹
Md. Akhtaruzzaman,² and Takahiro Namazu^{1,3*}

¹Kyoto University of Advanced Science, 18 Yamanouchigotanda-cho, Ukyo, Kyoto 615-8577, Japan

²The Islamic University of Madinah, Madinah 42351, Saudi Arabia

³Tohoku University, 2-1-1 Katahira, Aoba-ku, Sendai 980-8577 Japan

(Received October 15, 2025; accepted December 4, 2025)

Keywords: Al/Ni exothermic reaction, wafer bonding, four-point bending test, fracture strength

We describe the strength and fracture of Si wafers instantaneously bonded by exothermic reaction in an Al/Ni multilayer film. The Al/Ni multilayer film deposited by dual-source direct current (DC) sputtering is used as a heat source for the solder bonding of Si wafers. To reduce the numbers of voids and microcracks produced at the solder-reacted NiAl interface and the reacted NiAl layer, respectively, Al/Ni multilayer films are modified. By depositing the Al/Ni multilayer film with Ni layers on the top and bottom surfaces onto the base-side Si wafer, the number of voids at the base-side solder and reacted NiAl interface is reduced. Using a self-standing Al/Ni multilayer sheet with Ni layers on both sides reduces the number of microcracks introduced into the reacted NiAl layer. After dicing the bonded wafer to make a miniature rod having the bonded section, a four-point bending test is conducted. The improvements of the bonded section provide high fracture strength. The mechanical test determines the weakest portion of the bonded section. The effectiveness of modifying the Al/Ni reactive-bonding conditions is discussed, based on observations of fractured samples and results of energy-dispersive X-ray (EDX) analysis.

1. Introduction

Self-propagating exothermic reactions, which can be observed in multilayered metallic films composed of light and transition metals, have garnered significant attention as a novel heat source with unique exothermic characteristics that have never been seen before.^(1–8) For example, the heat of reaction per unit volume depends on the combination of atoms, atomic ratio, and bilayer thickness. The maximum temperature during the reaction depends on both the bilayer thickness and the entire volume. Additionally, the exothermic reaction rate depends on the bilayer thickness. That is, these exothermic characteristics can be controlled to their optimal levels in accordance with the intended applications of the film. The authors are utilizing this attractive functional material, Al/Ni multilayer film, as a heat source to instantaneously melt

*Corresponding author: e-mail: namazu.takahiro@kuas.ac.jp
<https://doi.org/10.18494/SAM5979>

solder for semiconductor wafer bonding.^(9–13) By applying a small amount of energy, such as an electric spark, to the Al/Ni multilayer film sandwiched between two Si wafers with a solder layer, the Si die attachment can be completed within 1 s. No significant electrical power is required, and no emissions are generated during the reaction, making the Al/Ni reactive-bonding technique an eco-friendly semiconductor-die-attach technology. It can help address the issue of global warming. However, for the practical application of the technique in semiconductor die attachment, several technical issues must be addressed. One of the issues is to reduce the number of voids produced in the bonded system after the reaction.⁽⁹⁾ Another approach is to reduce the number of cracks introduced into the reacted NiAl layer during the reaction.⁽¹⁰⁾ These defects would deteriorate the reliability of the bonded system.

In this research, we focus on reducing the numbers of voids and cracks produced in the bonded system after Al/Ni reactive bonding. Al/Ni multilayer films are modified for this purpose, and a four-point bending test demonstrates the effectiveness of the modification in reducing the numbers of voids and cracks, as evidenced by a comparison of the fracture strengths of the bonded samples under different conditions. Fractured surface observations and energy-dispersive X-ray (EDX) analysis are conducted to investigate the fracture mechanism.

2. Experimental Procedure

Figure 1 shows the process of fabricating a four-point bending test sample through Al/Ni exothermic reaction with snapshots. First, an n-type Si (001) wafer with a thickness of 1.5 mm is prepared as a starting material. The wafer is cut to $10 \times 10 \text{ mm}^2$ and $10 \times 15 \text{ mm}^2$ by mechanical dicing for the cap and base wafers, respectively. Then, Cr and Ni, with thicknesses of 100 and

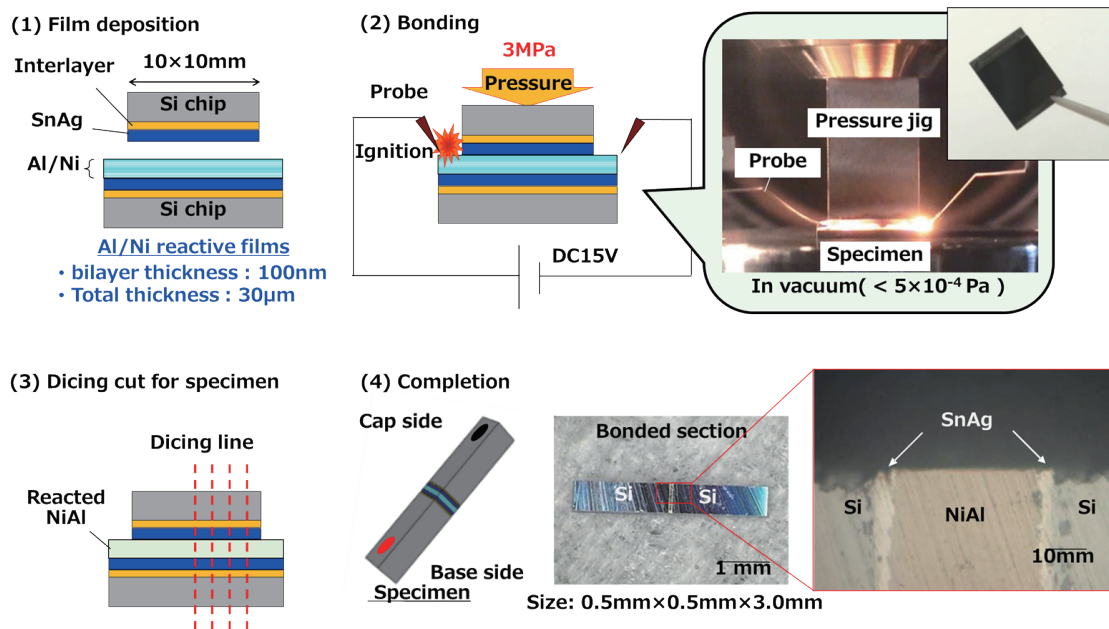


Fig. 1. (Color online) Process of fabricating four-point bending test sample through Al/Ni exothermic reaction.

500 nm, are sputtered onto both diced wafers as interlayers to improve the adhesion of the solder material to be deposited in the next step. SnAg with a thickness of 12 μm is deposited by co-sputtering onto the interlayer. After that, an Al/Ni multilayer film with a 1:1 atomic ratio and a 100 nm bilayer, indicating that 60 nm of Al and 40 nm of Ni are deposited alternately, is sputtered onto the solder layer on the base side. The first deposited layer is Al and the last one is Ni. The entire thickness of the Al/Ni multilayer film is 30 μm . After the depositions, the cap and base wafers are overlapped, facing each other. An electronic spark is applied to the Al/Ni multilayer film under a normal pressure of 3 MPa, applied from above in a vacuum. The reactive film ignites with bright orange light, and the solder bond is complete within a second. To prepare a sample for a four-point bending test, the bonded wafers are diced into a miniature rod with a cross-sectional area of $0.5 \times 0.5 \text{ mm}^2$. By polishing the entire surface of the rod to remove as many scratches as possible, the sample is prepared for the strength test. The sample features a bonded section at its center, comprising the two solder layers and the reacted NiAl layer. To distinguish the cap and base wafers, red and blue marks are applied to each side of the rod.

Figure 2 illustrates the three samples with different bonded sections, accompanied by corresponding cross-sectional photographs. Sample A is the standard sample in which an Al/Ni multilayer film is deposited on the base wafer, as explained above. The cross-sectional scanning electron microscopy (SEM) image reveals that vertical cracks were introduced into the reacted NiAl layer, and numerous voids were formed at the reacted NiAl and base-side solder interface. The NiAl–solder interface was formed immediately after the deposition of the Al/Ni multilayer film, which is referred to as the “deposition interface” here. Almost no voids were formed at the interface on the cap side, which is referred to as the “new-bonded interface” here. The differences in preparation conditions between the cap- and base-side interfaces are the contact materials between the reactive film and the solder, and the manner in which they were formed. Sample B is the first-step modified sample, whose top and bottom layers were composed of Ni, although the entire film composition slightly deviated from the 1:1 atomic ratio for Al and Ni. This means that the material in contact with SnAg was Ni at both interfaces. As shown in the SEM image,

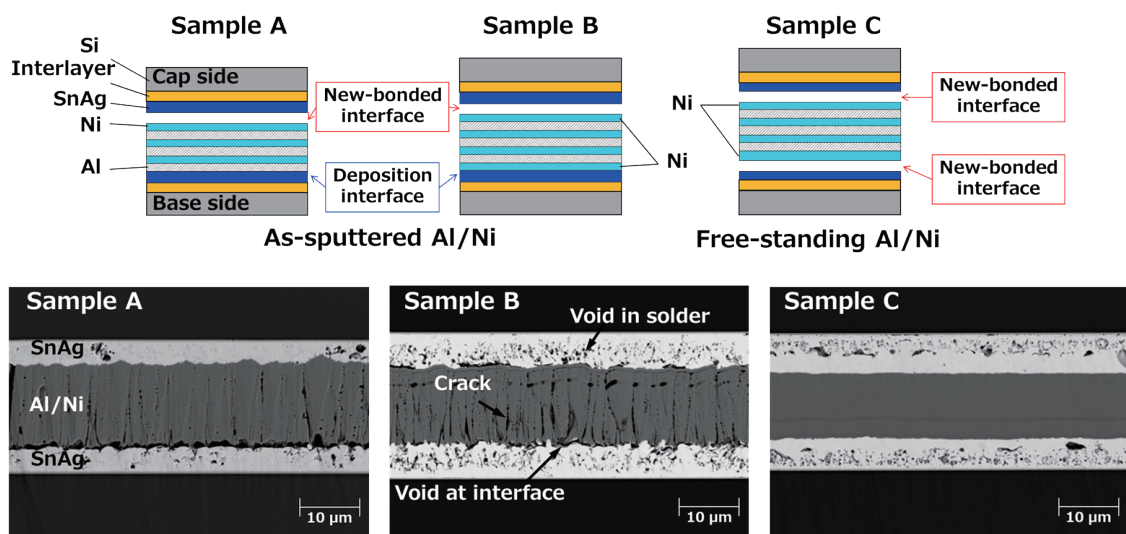


Fig. 2. (Color online) Sample configuration with cross-sectional SEM images.

the number of voids at the base-side interface has decreased. However, numerous cracks were created in the reacted NiAl layer compared with Sample A. Those cracks may have originated from an imbalance in mechanical restraint between the cap- and base-side interfaces during reactive bonding. Sample C is the second-step modified sample, in which a stand-alone Al/Ni multilayer film, whose top and bottom layers were composed of Ni, was sandwiched between the two Si wafers to eliminate the imbalance that likely occurred in Samples A and B. As seen in the SEM image, no visible voids or cracks are present. The differences between the three samples will result in various mechanical characteristics. The four-point bending test was performed using the original bending test equipment developed for microrod samples.^(11,12) All the tests were conducted in ambient environments.

3. Results and Discussion

Figure 3 shows the representative bending force–displacement curves of microrod samples, Samples A, B, and C. The force–displacement relationship for Sample A is linear until fracture at a bending force of around 1.5 N. Immediately after the fracture, the force immediately drops to zero, indicating that the introduced crack propagated rapidly until catastrophic failure was complete. That is, a brittle fracture occurred. Samples B and C show a similar trend to Sample A until the maximum force is applied. Still, their fracture force is found to be higher than that of Sample A. Note that, immediately after the fracture, the force did not immediately drop to zero but decreased gradually. This indicates that a crack propagated slowly toward a catastrophic fracture.

Figure 4 depicts the bending strengths of the three samples. The numbers of samples tested (N) were 3, 4, and 4 for Samples A, B, and C, respectively. The average bending strength was 18.1 MPa for Sample A, which is approximately one-half of the yield strength for the SnAg solder. For Samples B and C, the average bending strengths were 33.3 and 41.8 MPa, respectively, indicating that the outermost layer of Ni is efficacious in improving the mechanical strength of the jointed section. Additionally, it was confirmed that the use of a self-standing Al/Ni film

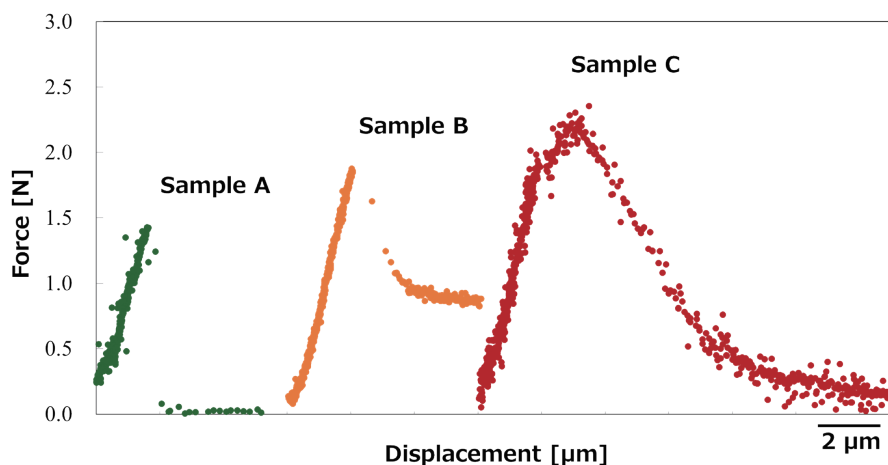


Fig. 3. (Color online) Representative bending force–displacement curves of Samples A, B, and C.

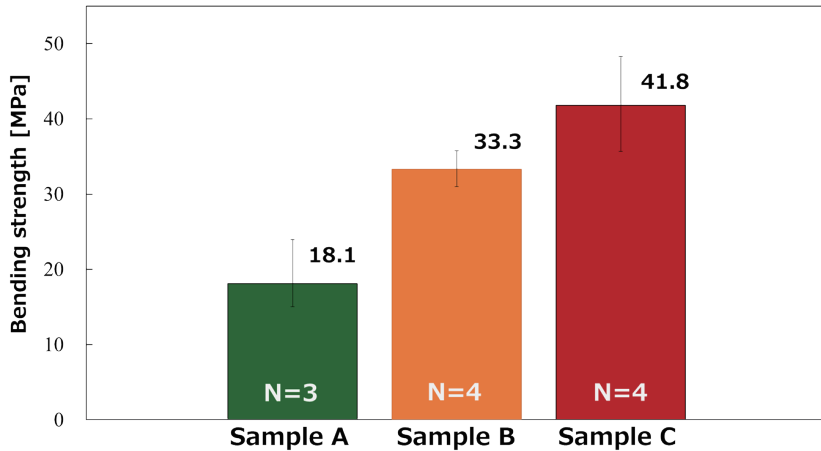


Fig. 4. (Color online) Bending strengths of Samples A, B, and C.

significantly affected strength. The representative optical microscopy results of fractured samples on the tensile stress application side after the strength test are shown in Fig. 5. It was confirmed that all the samples broke with crack initiation and opening, a Mode I fracture, on the side to which tensile stress was applied.⁽¹³⁾ Sample A fractured at the solder–NiAl interface on the base side, which was the weakest portion in the bonded system. The fractured surface was rough, indicating that many voids produced at the interface contributed to the fracture. Sample B failed at the solder–NiAl interface on the cap side, which is the opposite side in Sample A. The fractured surface appears rough. In Samples A and B, numerous vertical lines are visible in the reacted NiAl layer, which are cracks originating from approximately 12% volume shrinkage at the 1:1 atomic ratio during the exothermic reaction.⁽¹⁴⁾ They are caused by a mechanical restriction during reactive bonding. On the other hand, Sample C did not fracture at the NiAl–solder interface but fractured at the solder–Si wafer interface. The solder–NiAl interfaces were very smooth, unlike those of the other two samples, and no visible cracks were detected in the reacted NiAl layer. The use of a free-standing Al/Ni film for reactive bonding yielded these positive phenomena, leading to an improvement in the mechanical reliability of the Si wafer die attachment.

Figure 6 shows the EDX mapping results of the fractured surface for each sample. The arrows in the figure indicate the loading direction for each sample. In Sample A, the fracture surfaces on the cap and base sides exhibit green and red colors, respectively, indicating the presence of Al and Sn. Those colors are distributed entirely on each fracture surface, so the base-side solder and NiAl interface is apparently the weakest in the bonded system. This is caused by an incompatibility between Al and Sn, which is a combination that does not form any intermetallic compound.⁽¹⁵⁾ In Sample B, the cap- and base-side fracture surfaces consist of red and green colors, indicating Sn and Ni, respectively. The fracture occurred at the cap-side solder and NiAl interface, which differed from the base-side solder and NiAl interface in Sample A. This change is attributed to the higher compatibility between Sn and Ni, which would have suppressed void formation compared with the Sn-Al contact in Sample A. However, additional experiments are necessary to elucidate the mechanisms in detail. Note that the right-side corners

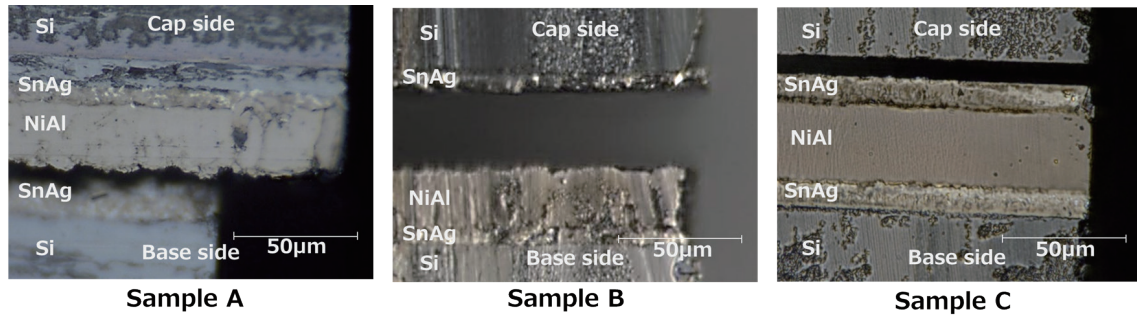


Fig. 5. (Color online) Optical microscopy images of fractured Samples A, B, and C.

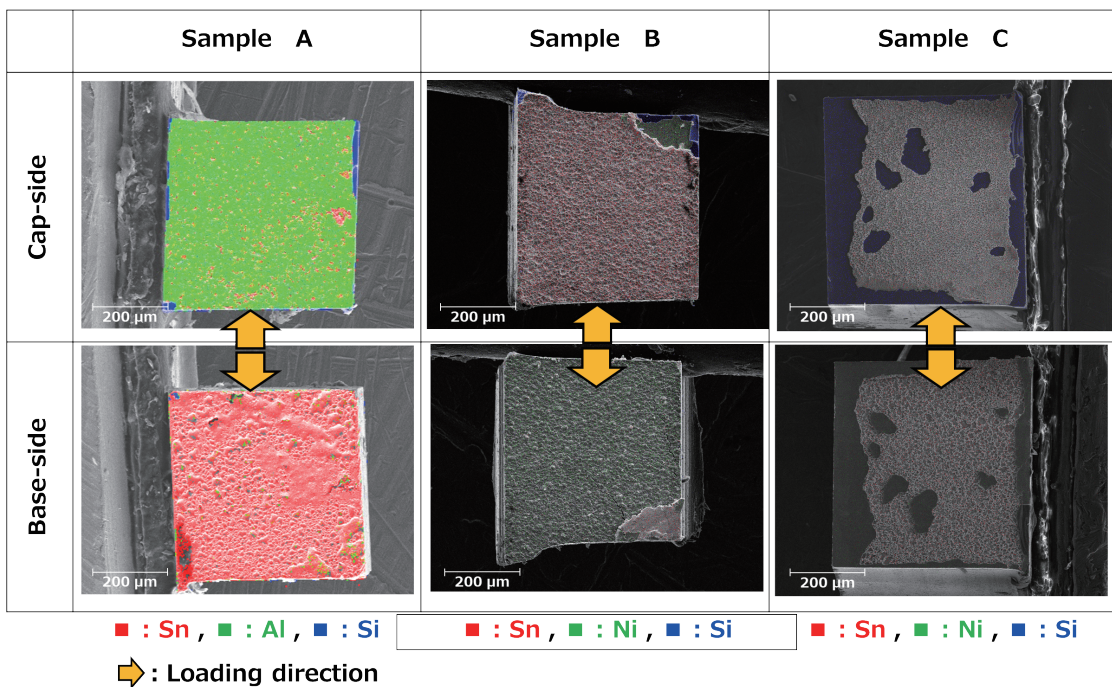


Fig. 6. (Color online) EDX mapping results of fractured surface for each sample.

of the fractured surface broke at another interface, implying that the weakness of the cap-side solder and NiAl interface was probably not so different from that of the other portions. In Sample C, the fractured surface appears more irregular. The cap-side surface is composed of blue and green colors, indicating Si and Ni, respectively, which is the interface between the cap-side Si wafer and the interlayer. From the experimental facts above, it was found that using a self-standing Al/Ni multilayer film with Ni layers on both sides strengthened the adhesion between the solder and reacted NiAl layers, and also the remaining NiAl layer did not adversely affect the strength of the bonded system.

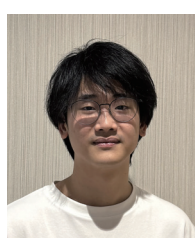
4. Conclusions

In this study, the strength of the bonded system prepared through Al/Ni exothermic reaction was investigated by the four-point bending test. On the basis of the observation results of the bonded system cross sections, Al/Ni multilayer films were modified step by step. The modifications appeared as a strength value, which was increased by adding Ni layers on both sides and by using a self-standing film. The fracture mechanism was discussed and concluded to have no adverse effect on the strength of the bonded system due to the remaining NiAl layer. This indicates that the Al/Ni reactive-bonding technique has potential as a future semiconductor die-attachment technology.

References

- 1 Z. A. Munir and U. Anselmi-Tamburini: Mater. Sci. Rep. **3** (1989) 277. [https://doi.org/10.1016/0920-2307\(89\)90001-7](https://doi.org/10.1016/0920-2307(89)90001-7)
- 2 B. K. Yen: J. Appl. Phys. **89** (2001) 1477. <https://doi.org/10.1063/1.1333027>
- 3 K. Blobaum, M. Reiss, J. Plitzko, and T. Weih: J. Appl. Phys. **94** (2003) 2915. <https://doi.org/10.1063/1.1598296>
- 4 X. Qiu and J. Wang: Sens. Actuators, A **141** (2008) 476. <https://doi.org/10.1016/j.sna.2007.10.039>
- 5 K. Maekawa, S. Ito, and T. Namazu: Jpn. J. Appl. Phys. **59** (2020) SII0. <https://doi.org/10.35848/1347-4065/ab769b>
- 6 T. Namazu, S. Ito, S. Kanetsuki, and S. Miyake: Jpn. J. Appl. Phys. **56** (2017) 06GN11. <https://doi.org/10.7567/JJAP.56.06GN11>
- 7 R. Fukuda and T. Namazu: J. Vac. Sci. Technol., B **43** (2025) 022801. <https://doi.org/10.1116/6.0004192>
- 8 T. Namazu, H. Takemoto, H. Fujita, Y. Nagai, and S. Inoue: Proc. 2006 IEEE 19th Int. Conf. Micro Electro Mechanical Systems (Istanbul, 2006) 286. <https://doi.org/10.1109/MEMSYS.2006.1627792>
- 9 S. Kanetsuki, K. Kuwahara, S. Egawa, S. Miyake, and T. Namazu: Jpn. J. Appl. Phys. **56** (2017) 06GN16. <https://doi.org/10.7567/JJAP.56.06GN16>
- 10 K. Maekawa, K. Kodama, S. Miyake, and T. Namazu: Jpn. J. Appl. Phys. **60** (2021) SCCL15. <https://doi.org/10.35848/1347-4065/abf39c>
- 11 T. Namazu, K. Ohtani, S. Inoue, and S. Miyake: ASME. J. Eng. Mater. Technol. **137** (2015) 031011. <https://doi.org/10.1115/1.4030413>
- 12 S. Miyake, K. Ohtani, S. Inoue, and T. Namazu: ASME. J. Eng. Mater. Technol. **138** (2016) 011006. <https://doi.org/10.1115/1.4032020>
- 13 S. Liu, Yuh J. Chao, and X. Zhu: Int. J. Solids Struct. **41** (2004) 6147. <https://doi.org/10.1016/j.ijisolstr.2004.04.044>
- 14 Roy W. Rice and William J. McDonough: J. Am. Ceram. Soc. **68** (1985) C-122. <https://doi.org/10.1111/j.1151-2916.1985.tb15328.x>
- 15 C. P. Wang, M. S. Wang, Y. L. Deng, J. B. Zhang, S. Y. Yang, Y. X. Huang, and X. J. Liu: J. Phase Equilib. Diffus. **43** (2022) 51. <https://doi.org/10.1007/s11669-022-00941-0>

About the Authors



Sarankamol Athichaikhongphat received his B.E. from Thammasat University, Thailand, in 2022 and is currently pursuing an M.E. degree at Kyoto University of Advanced Science (KUAS), Kyoto, Japan. His research interests include the development of mechanical characterization techniques for hard-coating thin-film materials and the measurement of the mechanical properties of materials used in MEMS and semiconductor devices. He is also interested in developing functional materials, such as shape-memory alloy and self-propagating exothermic films, through sputtering.



Kana Maekawa received her B.E. and M.E. degrees from Aichi Institute of Technology, Japan, in 2019 and 2021, respectively. In 2021, she was a visiting researcher at KUAS. Her research interest is in the application of Al/Ni exothermic films. She developed a laser ignition system for artificially controlling cracks in the reacted NiAl layer of the bonded system. She demonstrated that cracks introduced into the NiAl layer could be controlled by adjusting the ignition timing at multiple points.



Amit Banerjee received his M.Sc. (2009) and Ph.D. (2014) degrees from the Department of Physics at the Indian Institute of Technology Kanpur, India. He subsequently worked as a researcher at the City University of Hong Kong, Kyoto University, and the Japan Advanced Institute of Science and Technology. In September 2020, he joined the Graduate School of Engineering at Kyoto University as a junior associate professor. He has been working as an associate professor at KUAS since May 2025. He is interested in MEMS, NEMS, nanomechanics, and other emerging areas of micro- and nanoscience and technology. He is a recipient of the JSPS postdoctoral fellowship.



Md. Akhtaruzzaman received his B.Sc. and M.Sc. degrees in applied chemistry and chemical engineering from the University of Dhaka, Bangladesh, in 1996 and 1998, respectively, and his PhD degree from the Institute for Molecular Science (IMS), Okazaki, Japan, in March 2003. He is currently serving with the Department of Chemical Engineering at the Faculty of Engineering, Islamic University of Madinah (IU), Saudi Arabia. His research interests include the rational design of organic/inorganic semiconductors, nanomaterials, and device physics for various organic electronic device applications. He has published over 200 papers, reviews in peer-reviewed journals, patents, book chapters, and books.



Takahiro Namazu received his B.S., M.S., and Ph.D. degrees in mechanical engineering from Ritsumeikan University, Kusatsu, Japan, in 1997, 1999, and 2002, respectively. From 2002 to 2006, he served as an assistant professor in the Department of Mechanical and Systems Engineering at the Graduate School of Engineering, University of Hyogo, Himeji, Japan. In 2007, he was appointed as an associate professor at the same university. In 2010, he joined the Precursory Research for Embryonic Science and Technology program of the Japan Science and Technology Agency as a researcher. In 2016, he became a professor in the Department of Mechanical Engineering at Aichi Institute of Technology, Toyota, Japan. In 2020, he became a professor in the Faculty of Engineering at KUAS. Since 2025, he has been a professor at the International Center for Synchrotron Radiation Innovation Smart at Tohoku University, in a cross-appointed position. He is currently engaged in studies on functional film materials, such as self-propagating exothermic materials, and their applications to micro- and nano-electromechanical systems.

[\(namazu.takahiro@kuas.ac.jp\)](mailto:(namazu.takahiro@kuas.ac.jp))